Universiteit Leiden
The Netherlands

CD8+ T-cells in atherosclerosis: recognizing their contribution

Jong, M.J.M. de

Citation
Jong, M. J. M. de. (2025, January 23). *CD8+ T-cells in atherosclerosis: recognizing their contribution*. Retrieved from https://hdl.handle.net/1887/4177209

Version:	Publisher's Version
License:	Licence agreement concerning inclusion of doctoral thesis in the Institutional Repository of the University of Leiden
Downloaded from:	https://hdl.handle.net/1887/4177209

Note: To cite this publication please use the final published version (if applicable).


2

Chapter 2

Tc17 CD8$^+$ T-cells accumulate in murine atherosclerotic lesions, but do not contribute to early atherosclerosis development

Authors: J. van Duijn[1], M.J.M. de Jong[1], N. Benne[1], R.J.T. Leboux[1], M.E. van Ooijen[1], N. Kruit[1], A.C. Foks[1], W. Jiskoot[1], I. Bot[1], J. Kuiper[1], B. Slütter[1]

[1] Leiden Academic Centre for Drug Research, Division of BioTherapeutics, Leiden University, Einsteinweg 55, 2333 CC Leiden, The Netherlands.

Published in Cardiovascular Research 2021 Dec 17,
https://doi.org/10.1093/cvr/cvaa286

ABSTRACT

Introduction. $CD8^+$ T-cells can differentiate into subpopulations that are characterized by a specific cytokine profile, such as the Tc17 population that produces IL-17. The role of this $CD8^+$ T-cell subset in atherosclerosis remains elusive. In this study, we therefore investigated the contribution of Tc17 cells to the development of atherosclerosis.

Methods and Results. Flow cytometry analysis of atherosclerotic lesions from *Apoe*$^{-/-}$ mice revealed a pronounced increase in $ROR\gamma t^+$ $CD8^+$ T-cells compared to the spleen, indicating a lesion-specific increase in Tc17 cells. To study whether and how the Tc17 subset affects atherosclerosis, we performed an adoptive transfer of Tc17 cells or undifferentiated Tc0 cells into *Cd8a*$^{-/-}$*Ldlr*$^{-/-}$ mice fed a Western-type diet. Using flow cytometry, we showed that Tc17 cells retained a high level of IL-17A production *in vivo*. Moreover, Tc17 cells produced lower levels of IFN-γ than their Tc0 counterparts. Analysis of the aortic root revealed that the transfer of Tc17 cells did not increase atherosclerotic lesion size, in contrast to Tc0-treated mice.

Conclusion. These findings demonstrate a lesion-localized increase in Tc17 cells in an atherosclerotic mouse model. Tc17 cells appeared to be non-atherogenic, in contrast to their Tc0 counterpart.

TRANSLATIONAL PERSPECTIVE

$CD8^+$ T-cells are present in high numbers in human atherosclerotic plaques, however, their role in inflammation and the pathogenesis of atherosclerosis remains elusive. Our results indicate that the majority of $CD8^+$ T-cells in atherosclerotic plaques of mice have lost their ability to produce the pro-inflammatory cytokine IFN-γ and gain traits of IL-17-producing $CD8^+$ T-cells (Tc17 cells). We show that this subset of $CD8^+$ T-cells is less atherogenic than IFN-γ producing Tc1 cells.

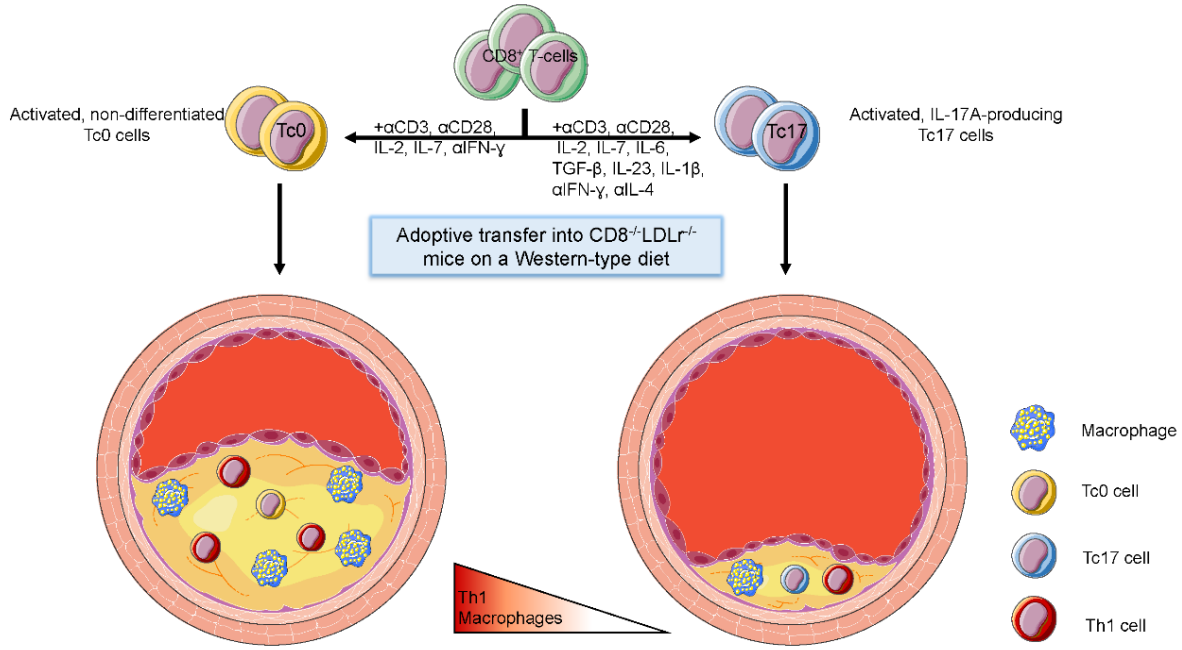

Graphical abstract

INTRODUCTION

Atherosclerosis, the most frequent underlying pathology of cardiovascular disease, is characterized by both the buildup of cholesterol as well as chronic inflammation within the wall of large- and medium-sized arteries. T-cells are observed in both early and advanced atherosclerotic lesions[1] and have been shown to contribute to lesion initiation and progression[2-4]. Different subsets of $CD4^+$ helper-T cells have been extensively described and studied in the context of atherosclerosis[5]. A pro-atherogenic function is ascribed to the interferon-γ (IFN-γ)-producing T helper 1 (Th1) subset[6, 7], whereas the interleukin (IL)-10-producing regulatory T cells (Tregs) are atheroprotective [8, 9]. The role of the Th2 subset, characterized by the production of IL-4 and IL-5, is more controversial. Whereas the signature Th2 cytokines IL-4, IL-5, and IL-33 are reported to inhibit atherosclerosis development [2, 10, 11], reduced Th2 responses and IL-4 deficiency were also reported to decrease lesion formation [12-14], suggesting a pro-atherogenic role for Th2 cells as well. Finally, the IL-17-producing Th17 subset is known to drive autoimmunity and atherogenesis via activation of the endothelium, increasing pro-inflammatory cytokine production, and contributing to macrophage recruitment [15-17]. In contrast, loss of suppressor of cytokine signaling (SOCS) 3 in T cells, resulting in increased IL-17 and IL-10 production, reduces atherosclerotic lesion development[18]. This effect is mediated via the induction of an anti-inflammatory macrophage phenotype and a reduction in vascular inflammation. Interestingly, treatment with recombinant IL-17 resulted in reduced expression of vascular cell adhesion molecule-1 (VCAM-1) as well as reduced T-cell infiltration in the lesions, suggesting the aforementioned atheroprotective effects of SOCS3 knockout are at least in part mediated via IL-17.

In a similar vein to their $CD4^+$ T-cell counterparts, $CD8^+$ T-cells can be categorized into subsets based on their cytokine production. Upon activation of $CD8^+$ T-cells, cytokines released by antigen-presenting cells (APCs) can influence the differentiation of the $CD8^+$ T-cells into different subsets. The cytokines IL-2 and IL-12 drive $CD8^+$ T-cells towards a Tc1 phenotype through the induction of the transcription factor T-box–containing protein expressed in T cells (T-bet) [19, 20]. Tc1 cells are known for their cytotoxic function and expression of effector molecules, such as granzymes, perforin, IFN-γ and TNF-α [21, 22]. These cells confer protection against intracellular infections [23, 24] as well as cancer [25]. Alternatively, the release of IL-4 by the APCs polarizes $CD8^+$ T-cells towards a Tc2 phenotype [26]. These cells express the transcription factor GATA3 and are characterized by the production of the cytokines IL-4, IL-5 and IL-13 [21, 26-28]. This cell type is known to propagate allergic reactions and contribute to autoimmune disorders, such as arthritis [29-31]. Finally, exposure to the cytokines IL-6, IL-21, and TGF-β drives $CD8^+$ T-cells to differentiate towards a Tc17 phenotype, by inducing the expression of the transcription factors RAR-related orphan nuclear receptor γt (RORγt) and interferon regulatory factor 4 [32, 33]. Tc17 cells are characterized by their production of IL-17 and have been shown to play a pro-inflammatory role in several autoimmune disorders, such as multiple sclerosis, diabetes and arthritis [21, 33-35].

The roles of $CD8^+$ T-cell subsets in atherosclerosis remain largely unexplored, although there are some studies suggesting that these cells may be involved. Tc1 cells have been implicated in atherogenesis, as IFN-γ-producing $CD8^+$ T-cells potentiated atherosclerosis development in apolipoprotein E deficient (*Apoe*$^{-/-}$) mice [36]. Additionally, IFN-γ produced by $CD8^+$ T-cells was shown to contribute to monopoiesis during early lesion development in low-density lipoprotein receptor-deficient (*Ldlr*$^{-/-}$) mice [37]. Moreover, *Apoe*$^{-/-}$ mice deficient in E3-ligase CBL-B showed an increase in INF-γ and granzyme B-producing $CD8^+$ T-cells, resulting in enhanced macrophage killing and atherosclerosis [38]. Finally, an increase in IL-17-producing $CD8^+$ T-cells in the circulation of humans has been associated with a higher incidence of myocardial

infarction [39], hinting at a role for Tc17 cells in cardiovascular disease. However, direct evidence showing a causal relation between Tc17 cells and atherosclerosis is lacking.

Here, we systematically investigated the presence of different CD8$^+$ T-cell subsets in a murine model of atherosclerosis and observed an increase in the number of Tc17 cells within the lesions. We show that undifferentiated CD8$^+$ T-cells switch to a Tc1 phenotype when transferred into *Ldlr*$^{-/-}$ mice on a Western-type diet (WTD). CD8$^+$ T-cells that are polarized towards Tc17 cells, however, produced lower levels of IFN-γ upon adoptive transfer and showed to be non-atherogenic. Tc0 cells, on the other hand, produced high levels of IFN-γ and enhanced atherosclerotic lesion formation.

MATERIALS AND METHODS

Mice. C57Bl/6, *Cd8a*$^{-/-}$, *Ldlr*$^{-/-}$ and *Apoe*$^{-/-}$ mice were purchased from Jackson Laboratory (Bar Harbor, Maine, USA) and bred in-house. *Cd8a*$^{-/-}$ mice were crossed with *Ldlr*$^{-/-}$ mice to obtain *Cd8a*$^{-/-}$ *Ldlr*$^{-/-}$ mice in-house, after which genotypes were verified by PCR. The mice were kept under standard laboratory conditions and food and water were provided *ad libitum*. For the development of advanced atherosclerotic lesions in *Apoe*$^{-/-}$ mice, mice were kept on a chow diet for 35–49 weeks before analysis of CD8$^+$ T-cell phenotypes in the lesion. Upon sacrifice, mice were subcutaneously anesthetized with a lethal dose of ketamine (40 mg/mL), sedazine (8 mg/mL) and atropine (0.1 mg/mL). All animal work was performed in compliance with the Dutch government guidelines and the Directive 2010/63/EU of the European Parliament. Experiments were approved by the Ethics Committee for Animal Experiments of Leiden University.

Cell preparation and flow cytometry. Mice were sacrificed as described above and blood, spleens, and aortas were harvested after *in situ* perfusion with phosphate-buffered saline (PBS, pH 7.4, Lonza). White blood cells were obtained by lysing blood samples two times for 2 min with lysis buffer (0.15 M NH_4Cl, 1 mM $KHCO_3$, 0.1 mM Na_2EDTA; pH 7.3). Single-cell suspensions of spleens were obtained by using a 70-μm cell strainer (Greiner Bio-One). Splenocytes were lysed for 1 min with lysis buffer to obtain white blood cells. Aortas were cleaned of perivascular fat, cut into small pieces, and digested by incubation with a digestion mix (collagenase I 450 U/mL, collagenase XI 250 U/mL, DNAse 120 U/mL, and hyaluronidase 120 U/mL; all Sigma-Aldrich) for 30 min at 37°C while shaking, and subsequently strained over a 70-μm strainer. Cells were stained with the appropriate antibodies (Suppl. Table 1). For intracellular staining, cells were fixed and permeabilized by using an intracellular staining kit (eBioscience) according to the manufacturer's protocol. To detect cytokine production, cells were stimulated for 3.5 hours with phorbol 12-myristate 13-acetate (PMA, 50 ng/mL, Sigma-Aldrich) and ionomycin (500 ng/mL, Sigma-Aldrich) in the presence of brefeldin A (ThermoScientific) in complete RPMI 1640 medium containing 25 mM HEPES (Lonza) supplemented with 5% fetal bovine serum (Greiner), 60 μM β-mercaptoethanol (Sigma), 100 U/mL mix of penicillin/streptomycin (Lonza), 1% non-essential amino acids (NEAA; Gibco), 1% sodium pyruvate (Sigma), and 2% L-glutamine (Lonza) at 37°C and 5% CO_2. Flow cytometry analyses were performed on a Beckman Coulter Cytoflex S and FlowJo software (Treestar).

In vitro culture of Tc0 and Tc17 cells. Spleens, mesenteric lymph nodes, and iliac lymph nodes were isolated from C57Bl/6 mice after cervical dislocation. CD8$^+$ T-cells were isolated by using a negative selection magnetic CD8$^+$ T-cell isolation kit (Milteny Biotec) according to the manufacturer's protocol. $0.3*10^6$ cells were plated per well in a 96-well plate in a total volume of 200 μL complete RPMI (as stated above). In order to obtain undifferentiated Tc0 cells, the medium was supplemented with 20 U/mL IL-2 (Peprotech), 0.5 ng/mL IL-7 (Peprotech), 0.5

µg/mL soluble anti-CD3 (ThermoScientific), 0.5 µg/mL soluble anti-CD28 (ThermoScientific) and 10 µg/mL anti-IFN-γ (BioXcell). For Tc17 differentiation, the medium was supplemented with 20 U/mL IL-2 (Peprotech), 0.5 ng/mL IL-7 (Peprotech), 20 ng/mL IL-6 (Peprotech), 5 ng/mL TGF-β (BioLegend), 20 ng/mL IL-1β (Peprotech), 20 ng/mL IL-23 (R&D systems), 0.5 µg/mL soluble anti-CD3 (ThermoScientific), 0.5 µg/mL soluble anti-CD28 (ThermoScientific), 10 µg/mL anti-IL-4 (BioXcell) and 10 µg/mL anti-IFN-γ (BioXcell). The cells were incubated for two days at 37°C and 5% CO_2, after which the medium was refreshed with the same cytokine stimulations, but without anti-CD3 and anti-CD28. The cells were incubated for one more day before analysis by flow cytometry or adoptive transfer.

RNA isolation and qPCR. RNA was isolated from *in vitro* cultured Tc0 and Tc17 cells by phenol/chloroform extraction. cDNA was synthesized using Maxima H minus reverse transcriptase reagents (ThermoFisher, Bleiswijk, the Netherlands) according to the manufacturer's protocol. After creating cDNA, the SensiMix SYBR low-ROX kit (GC Biotech, Waddinxveen, the Netherlands) was used to perform the quantitative PCR (qPCR). The primers used for the qPCR are listed in supplementary table 2. The PCR was run under the following conditions: initial denaturation 10 min at 95°C, followed by denaturation at 95°C for 15 seconds and annealing/extension at 64°C for 40 seconds for 40 cycles. The transcription levels were normalized to the expression of β-actin.

Adoptive transfer. Blood samples of 100 µL were drawn via the tail vein in EDTA-containing tubes (Sarstedt) from 18 *Cd8a*$^{-/-}$*Ldlr*$^{-/-}$ mice between 8 and 14 weeks of age. Total cholesterol levels were assessed by using an enzymatic colorimetric assay (Roche Diagnostics). The mice were randomized into two groups based on age, weight, and plasma cholesterol levels. From the start of the experiment, mice were fed a Western-type diet (WTD) containing 0.25% cholesterol and 15% cocoa butter (Special Diet Services, Witham, Essex, UK) for 6 weeks. Every week, mice received intravenous injections of matched numbers of between $8.8*10^5$ and $2.3*10^6$ Tc0 or Tc17 cells, depending on the amount obtained during isolation (on average $1.7*10^6$ per injection). During the experiment, transfer efficiency was monitored by drawing blood after 2 and 4 injections of $CD8^+$ T-cells, 5 days after the mice received the last injection. The mice were sacrificed one week after the sixth injection as described above, and organs were isolated as described under *cell preparation and flow cytometry*.

In vitro Dendritic cell culture. Bone-marrow from *Ldlr*$^{-/-}$ and *Cd8a*$^{-/-}$*Ldlr*$^{-/-}$ mice was isolated and cultured in DMEM containing 25 mM HEPES (Lonza) supplemented with 5% fetal bovine serum (Greiner), 60 µM β-mercaptoethanol (Sigma), 100 U/mL mix of penicillin/streptomycin (Lonza), 1% L-glutamine (Lonza), and 20ng/ml GM-CSF (Invitrogen) at 37°C and 5% CO_2. After 8 days, dendritic cells (DCs) were transferred to a 96-wells plate in a density of 20.000 cells/well and exposed to 0, 0.1, 1, 10 or 100 µg/ml ovalbumin and 1 ng/ml lipopolysaccharide for 24 hours. 24 hours after DC activation, ovalbumin specific $CD8^+$ T-cells were labeled with CFSE (Sigma) and were cocultured with the DCs in a DC:$CD8^+$ T-cell ratio of 1:5 for 72 hours. After 72 hours, $CD8^+$ T-cell expansion was evaluated by FACS analysis.

Cross-presentation in vivo. 5 *Ldlr*$^{-/-}$ and 5 *Cd8a*$^{-/-}$*Ldlr*$^{-/-}$ mice received an adoptive transfer of 50.000 ovalbumin specific OTI $CD8^+$ T-cells. 24 hours after the adoptive transfer, the mice were vaccinated with 100 µg ovalbumin and 50 µg poly I:C dissolved in PBS subcutaneously. One week after vaccination, the spleens were taken for FACS analysis, to evaluate $CD8^+$ T-cell expansion.

Histological analysis. All hearts were embedded in optimal cutting temperature (O.C.T.) compound (Sakura) and horizontally sectioned towards the aortic axis and the aortic arch. Upon reaching the aortic root, defined by the trivalve leaflets, 10 µm sections were collected. Lesion

size analysis was performed on cryosections of the aortic root lesion stained with Oil-red O and hematoxylin (Sigma-Aldrich). Sirius Red staining (Sigma-Aldrich) was performed on corresponding sections to determine collagen content, and Masson's Trichrome staining (Sigma-Aldrich) to determine the necrotic area. Plaque macrophages were stained immunohistochemically by using a rat anti-mouse Monocytes/Macrophages antibody (MOMA, 1:1000, AbD Serotec) as a primary antibody, biotinylated rabbit anti-rat IgG (1:100; Vector) as a secondary antibody, and Vectastain ABC horseradish peroxidase in combination with ImmPACT Nova Red for visualization (Vector). Plaques were stained for VCAM-1 by using purified rat anti-mouse CD106 (1:100, BD Biosciences) as a primary antibody, biotinylated rabbit anti-rat IgG (1:200, Vector) as a secondary antibody and Vectastain ABC horseradish peroxidase in combination with ImmPACT Nova Red for visualization (Vector). The average plaque size (in μm^2) was calculated from five sequential sections. For all other analyses, three subsequent sections displaying the highest plaque content per mouse were analyzed. All microscopic analyses were performed on a Leica DM-RE microscope using Leica QWin software and were blinded for independent analysis. The relative amount of collagen, macrophages, and necrosis in the atherosclerotic lesions was quantified by dividing the area stained positive for collagen, MOMA or that displaying necrosis by the total lesion surface area, and calculated as a percentage.

Statistical analysis. The data are presented as individual dot plots with bars denoting the mean, and the number of animals in each group is stated in the text. Data were tested for normal distribution by using a Shapiro-Wilk normality test and analyzed by using a two-tailed Student's *t*-test, Mann–Whitney test, one-way or two-way ANOVA, as appropriate. Statistical analysis was performed using Prism (GraphPad). Probability values of $P< 0.05$ were considered significant.

RESULTS

Increased expression of RORγt by CD8$^+$ T-cells derived from advanced murine atherosclerotic lesions.

We investigated the presence of the different CD8$^+$ T-cell subsets in the atherosclerotic lesions of *Apoe*$^{-/-}$ mice with advanced atherosclerosis using flow cytometry. We focused on the difference in phenotype between CD8$^+$ T-cells derived from the aortic lesions and their counterparts in the spleen, as these cells can locally affect the lesion development and composition. We observed a significant decrease in the percentage of CD8$^+$ T-cells that produce IFN-γ within the lesions compared to their counterparts in the spleen (11.7 % vs 39.3 %, Figure 1A, representative FACS plots in Suppl. Figure 1). This is in line with our previous research, showing a reduced number of cytokine-producing CD8$^+$ T-cells in the lesions of these mice, probably due to the immunosuppressive effects of increased CD39-expression on these cells[40]. We were unable to detect any IL-4 secretion by aortic CD8$^+$ T-cells, whereas we did detect low levels of this cytokine in the splenic CD8$^+$ T-cells (Figure 1B). Conversely, we observed no production of IL-5 by splenic CD8$^+$ T-cells, whereas there was a low expression of this cytokine in their aortic counterparts (Figure 1C). Finally, we observed only very low expression levels of IL-17A in the CD8$^+$ T-cells derived from both sites, with no significant differences between the different sites (Figure 1D) and no production of IL-10 was detected (Figure 1E). Due to the low cytokines levels, we looked into the expression of the key transcription factors associated with the different Tc subsets in the lesions of these mice: T-bet, GATA3, RORγt, and FOXP3 for Tc1, Tc2, Tc17, and regulatory CD8$^+$ T-cells (TcReg), respectively. Interestingly, we observed a significant 45-fold increase in the percentage of CD8$^+$ T-cells that are positive for RORγt (Figure 1G),

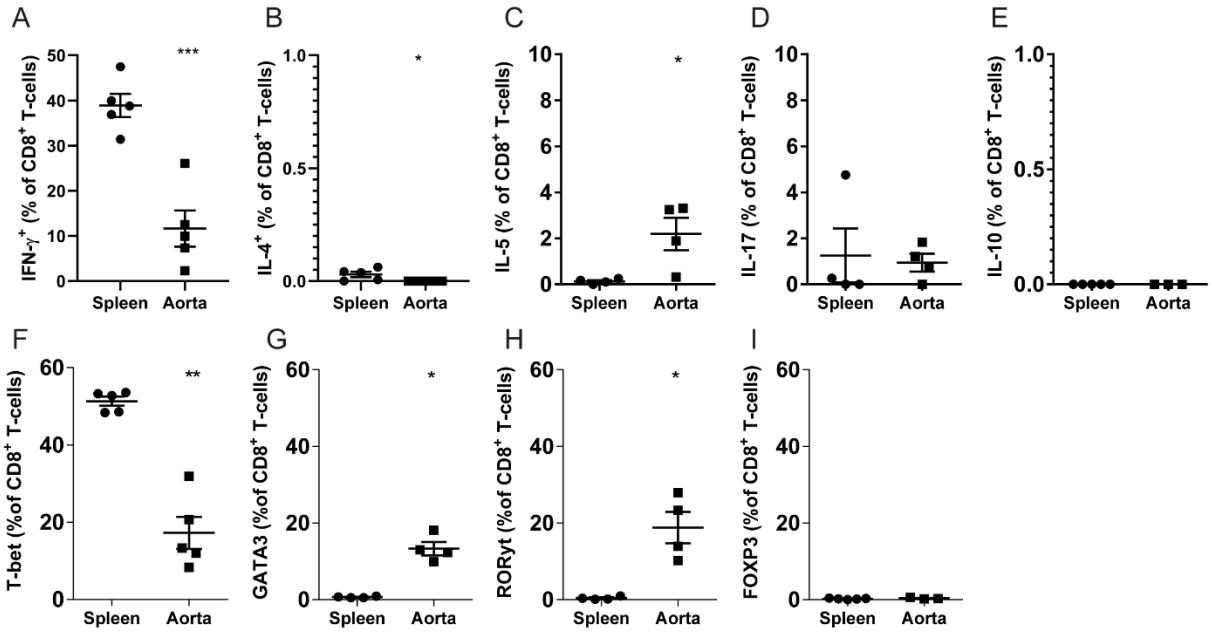

Figure 1. Murine atherosclerotic lesions display an increased expression of the Tc17-associated transcription factor RORγt, as well as the Tc2-associated transcription factor GATA3 within the CD8$^+$ T-cell compartment compared to the spleen. Flow cytometric analysis of IFN-γ$^+$ (A), IL-4$^+$ (B), IL-5$^+$ (C), IL-17A$^+$ (D), IL-10$^+$ (E), T-bet$^+$ (F), GATA3$^+$ (G), RORγt$^+$ (H) and FOXP3 (I) CD8$^+$ T-cells in the aortas and spleens of *Apoe*$^{-/-}$ mice stimulated for 3.5 h with PMA and ionomycin. Cells were pre-gated on live, Thy1.2$^+$ CD8$^+$ T-cells. Representative FACS plots are available in Suppl. Figure 1. Individual data points and mean ± SEM of n = 5 (A, B, F), n = 4 (C, D, G, H), or n = 3 (E, I) *Apoe*$^{-/-}$ mice of 35 to 49 weeks old, data are representative of n=3 independent experiments. Significance was determined by using an unpaired *t*-test (A, C) or a Mann-Whitney test (B, D, E, F, G, H, I). *P < 0.05, **P < 0.01, ***P < 0.001.

as well as a 19-fold increase in the percentage of GATA3-expressing CD8$^+$ T-cells (Figure 1F) and an almost 2-fold increase in FOXP3 positive CD8$^+$ T-cells in the aorta compared to the spleen (Figure 1H), whereas the percentage of T-bet-expressing CD8$^+$ T-cells showed a 3-fold decrease (Figure 1E). Of note, we only observed IFN-γ production by the T-bet positive CD8$^+$ T-cells in the aorta, but not by the RORγt or GATA3-expressing CD8$^+$ T-cells (Suppl. Figure 1), confirming functionally distinct lineages. As there was such a pronounced increase in the RORγt-expressing lesional CD8$^+$ T-cells, we set out to further explore the role of Tc17 cells in atherosclerosis.

In vitro characterization of Tc0 and Tc17 cells.

To evaluate the role of Tc17 cells in atherosclerotic lesion development, we decided to perform an adoptive transfer of Tc17 cells into *Cd8a*$^{-/-}$*Ldlr*$^{-/-}$ mice. First, we cultured undifferentiated CD8$^+$ T-cells (Tc0) and Tc17 cells *in vitro*, based on previously published protocols[33,41,42]. CD8$^+$ T-cells were isolated from wild-type mice and activated by using anti-CD3 and anti-CD28 antibodies. Tc0 were cultured for three days in medium supplemented with IL-2, IL-7, and anti-IFN-γ. Tc17 cells were differentiated for three days in medium supplemented with IL-2, IL-7, IL-6, IL-1β, TGF-β, IL-23, anti-IL-4, and anti-IFN-γ. Flow cytometry analysis revealed that our approach led to a robust Tc17 phenotype, with a 19-fold increase in the percentage of cells positive for IL-17A in the Tc17 cells compared to the Tc0 cells (24.8% vs 1.3%, Figure 2A, representative FACS plots shown in Suppl. Figure 2),

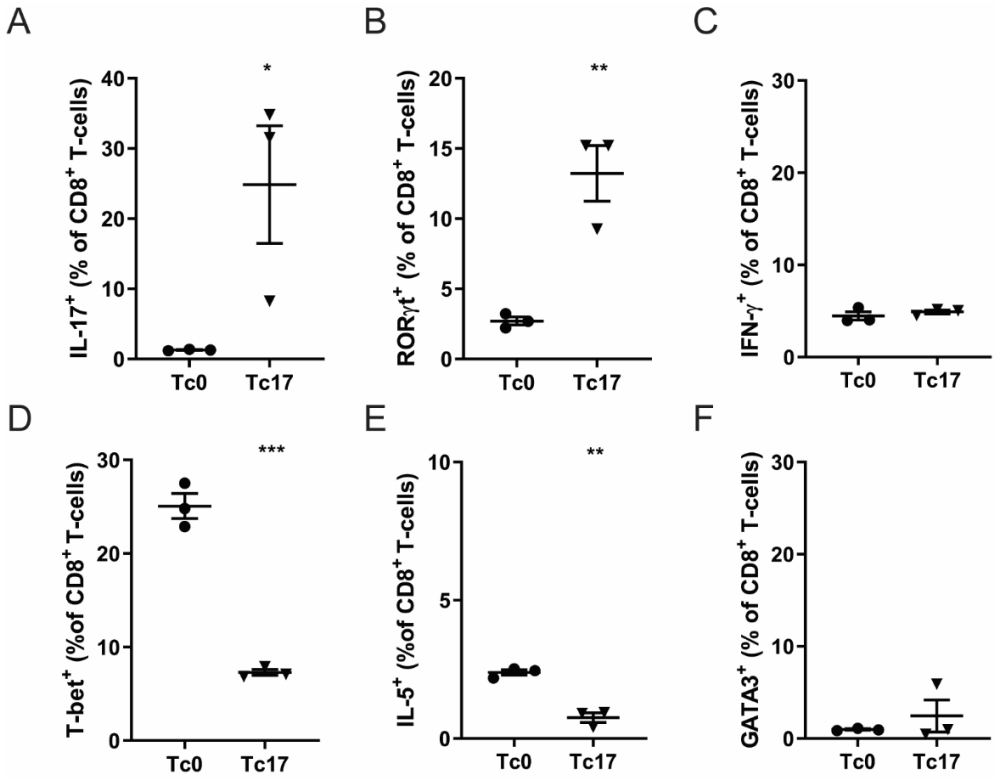

Figure 2. Tc0 and Tc17 cells demonstrate phenotypical differences in cytokine production and transcription factor expression. Flow cytometric analysis of IL-17A$^+$ (A), RORγt$^+$ (B), IFN-γ$^+$ (C), T-bet$^+$ (D), IL-5$^+$ (E) and GATA3$^+$ (F) CD8$^+$ T-cells isolated from C57Bl/6 mice and polarized for 3 days into Tc0 or Tc17 cells. Cells were stimulated for 3.5 h with PMA and ionomycin and pre-gated on live, Thy1.2$^+$ CD8$^+$ T-cells. Representative FACS plots are available in Suppl. Figure 2. Individual data points and mean ± SEM of n = 3, representative of n=3 experiments. Significance was determined by using an unpaired *t*-test. *P < 0.05, **P < 0.01, ***P < 0.001.

associated with a 5-fold increase in RORγt-expressing cells (13.2% vs. 2.7%, Figure 2B), and a reduction in T-bet-expressing cells (7.3% vs. 25.1%, Figure 2D). Moreover, both Tc0 and Tc17 produced low amounts of IFN-γ (4.5% and 4.9%, respectively, Figure 2C), indicating that these cells do not display a Tc1 phenotype. We observed a low production of IL-5 by both subsets, although the Tc0 subset produced 3-fold more IL-5 compared to the Tc17 subset (2.4% vs. 0.8%, Figure 2E). The percentage of GATA3$^+$ cells was low in both groups and did not differ between the two subsets (Figure 2F), indicating the cultured cells do not display a Tc2 phenotype. Finally, we confirmed the Tc17 phenotype on transcriptional level and show increased expression of RORγt and CCR6, another established Th17 marker (Suppl. Figure 3).

Adoptively transferred CD8$^+$ T-cells cells migrate to the atherosclerotic lesion and affect the local CD4$^+$ T-cell population.

To determine the effect of Tc17 cells on the development of atherosclerosis, *in vitro* cultured Tc0 or Tc17 cells were adoptively transferred into *Ldlr$^{-/-}$* mice that were also deficient in CD8$^+$ (*Cd8a$^{-/-}$Ldlr$^{-/-}$* mice) and therefore had no endogenous CD8$^+$ T-cell population (Suppl. Figure 4A, overview of experimental setup: Suppl. Figure 4B). Beside the absence of CD8$^+$ T-cells in these mice, the composition of blood leukocytes in *Cd8a$^{-/-}$Ldlr$^{-/-}$* mice was comparable to that of *Ldlr$^{-/-}$* mice (Suppl. Figure 5A), with only minor changes in monocyte activation (Suppl. Figure 5B).

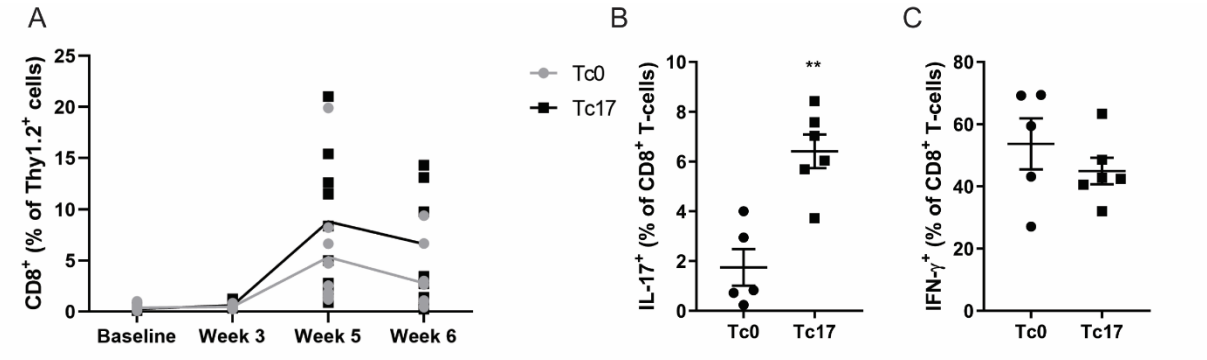

Figure 3. CD8$^+$ T-cell populations increase over time upon adoptive transfer in both treatment groups. (A) Analysis of percentages of CD8$^+$ T-cells in the blood of the *Cd8a$^{-/-}$Ldlr$^{-/-}$* mice after 2 and 4 injections of Tc0 or Tc17 cells and at sacrifice. Cells were pre-gated on live, Thy1.2$^+$ cells, mean ± SEM. (B) IL-17A and (C) IFN-γ production by the CD8$^+$ T-cells in the blood after 4 injections, as analyzed by flow cytometry. Cells were stimulated for 3.5 h with PMA and ionomycin and pre-gated on live, Thy1.2$^+$ CD8$^+$ T-cells. Individual data points and mean ± SEM, n=9 mice per group. Significance was determined by using a two-way ANOVA with Bonferroni's multiple comparisons (A) or by using an unpaired *t*-test (B, C). *P < 0.05, **P < 0.01, ***P < 0.001.

Deletion of CD8a may also result in the ablation of CD8$^+$ dendritic cells (DCs). Although, CD8$^+$ DCs have a dominant role in antigen cross-pre- sentation,43 DCs from *Cd8a$^{-/-}$Ldlr$^{-/-}$* were able to induce CD8$^+$ T-cell expansion to a similar extent as DCs from *Ldlr$^{-/-}$* mice, after exposure to ovalbumin in vivo and in vitro (Figure S5C and D). This suggests cross-presentation in *Cd8a$^{-/-}$ Ldlr$^{-/-}$* mice is not impaired. In line with reports in CD8$^+$ deficient *Apoe$^{-/-}$* mice [44, 45], atherosclerotic lesion development was not affected by ablation of CD8$^+$ T-cells, as atherosclerotic lesions were comparable in size and composition after feeding *Ldlr$^{-/-}$* mice and *Cd8a$^{-/-}$Ldlr$^{-/-}$* mice (age 8-15 weeks) a western type diet for 6 weeks (Suppl. Figure 5 E, F, G) .

The adoptive transfer with *in vitro* expanded Tc0 (control group) or Tc17 (treatment group) cells resulted in an increase in the CD8$^+$ T-cell population in the blood of both treatment groups over time (Figure 3A). At four weeks post the first adoptive transfer, the circulating CD8$^+$ T-cells in the Tc17-treated group showed a substantially (4-fold) increased production of IL-17A compared to those in the Tc0-treated group (6.4% vs 1.7%, Figure 3B), suggesting a stable Tc17 phenotype. Interestingly, we observed plasticity in the Tc0 subset, as these cells showed an increase in IFN-γ production from 4.5% at baseline to 53.6% four weeks after the first transfer. The Tc17 cells also showed an increased IFN-γ production from 4.9% to 44.9% (Figure 2C, 3C). Therefore, we analyzed the relative amount of splenic IFN-γ$^+$ CD8$^+$ T-cells at sacrifice. Again, we observed that in the Tc0-treated group a larger fraction of the cells produce IFN-γ (75.9%) compared to those in the Tc17-treated group (30.5%, Figure 4A,C), although in both groups the percentage of IFN-γ$^+$ cells was notably higher than directly after *in vitro* differentiation (Figure 2C). In line with our expectations, the Tc17-treated group still displayed more IL-17A$^+$ cells as compared to the Tc0 group (7.6% vs 2.2%, Figure 4B,C), albeit less compared to the *in vitro* cytokine production levels at the moment of injection (Figure 2A). Moreover, at sacrifice, 86.1% of CD8$^+$ T-cells in the Tc0 group expressed T-bet, whereas in the Tc17 group this comprised 46.1% of the total CD8$^+$ population (Figure 4D,F), suggesting the majority of the injected Tc0 cells had converted to a Tc1 phenotype. We observed a non-significant 1.2-fold increase in RORγt expression in the Tc17-treated group compared to the controls (Figure 4E,F). Of note, the adoptively transferred CD8$^+$ T-cells were able to proliferate *in vivo*, as we observed 30.2% and 20.0% Ki-67 expression in the Tc0 and Tc17 group, respectively (Figure 4G,I). No differences were observed in the percentage of FoxP3$^+$ CD8$^+$ T-cells between the different groups (Suppl. Figure 4C).

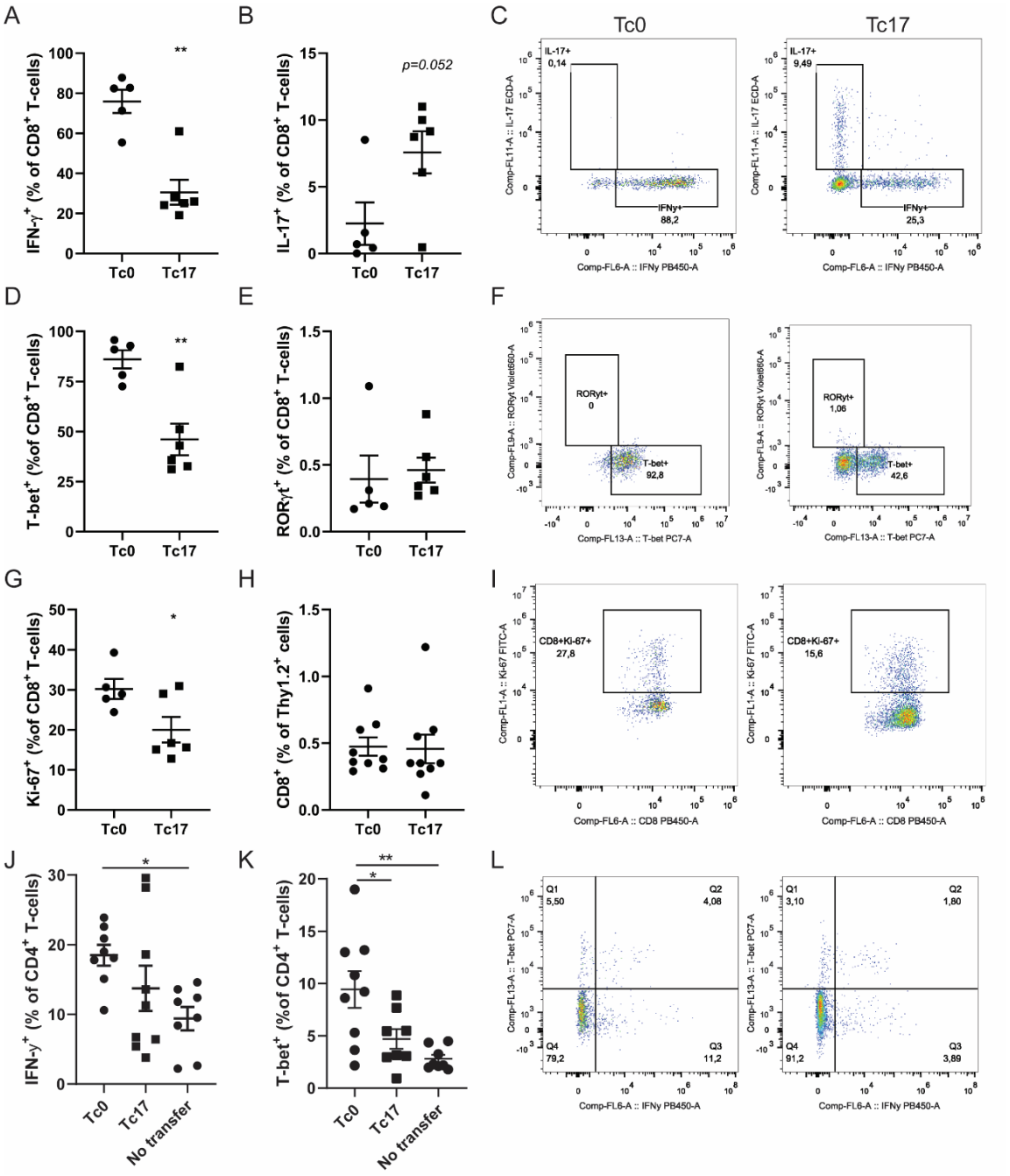

Figure 4. Adoptive transfer of Tc17 cells in *Cd8a*$^{-/-}$*Ldlr*$^{-/-}$ mice skews the CD4$^+$ T-cells towards a less inflammatory phenotype in the aortic microenvironment. Flow cytometric analysis of IFN-γ$^+$ (A), IL-17A$^+$ (B) T-bet$^+$ (D) RORγt$^+$ (E), and Ki-67$^+$ (G) CD8$^+$ T-cells in the spleens of the *Cd8a*$^{-/-}$*Ldlr*$^{-/-}$ mice that received the adoptive transfer of Tc0 or Tc17 cells at the time of sacrifice. Representative FACS plots are shown in (C,F,I). The gating of cytokine-positive populations was based on unstimulated controls. Cells were pre-gated on live, Thy1.2$^+$ CD8$^+$ T-cells. (H) percentages of CD8$^+$ T-cells in the aortas of the *Cd8a*$^{-/-}$*Ldlr*$^{-/-}$ mice at the time of sacrifice, analyzed by flow cytometry. Cells were pre-gated on live, Thy1.2$^+$ cells. Flow cytometry analysis of IFN-γ$^+$ (J) and T-bet$^+$ (K) CD4$^+$ T-cells in the aortas of the *Cd8a*$^{-/-}$*Ldlr*$^{-/-}$ mice at the time of sacrifice. Representative FACS plots are shown in (L), cytokine-positive populations were gated based on unstimulated controls. Cells were pre-gated on live, Thy1.2$^+$ CD4$^+$ T-cells. Cells were stimulated for 3.5 h with PMA and ionomycin. Individual data points and mean ± SEM, n=9 mice per group. Significance was determined by using a Mann-Whitney test (A, B, D, G) or by using an unpaired *t*-test (C, E, F, H, I). *P < 0.05, **P < 0.01, ***P < 0.001.

In addition to the spleen and blood, we were able to detect $CD8^+$ T-cells in the aortic lesions of both Tc0- and Tc17-recipient mice at the time of sacrifice (Figure 4H), illustrating that the adoptively transferred $CD8^+$ T-cells migrate into the plaques. However, as the total number of lymphocytes within murine aortas is low, these numbers did not allow us to distinguish the different $CD8^+$ T-cell subsets. Interestingly, we did observe changes in the $CD4^+$ T-cell compartment in the lesion, showing a significant increase in IFN-γ production (Figure 4J,L $p<0.05$) and T-bet expression (Figure 4K,L $p<0.05$) in the Tc0-treated group, suggesting a skewing towards an inflammatory Th1 phenotype. This Th1 skewing effect was minimal and not statistically different after Tc17 transfer (Figure 4J,K,L).

Adoptive transfer of Tc17 cells does not accelerate atherosclerotic lesion development in CD8-deficient atherosclerotic mice.

We next assessed how the adoptive transfer of $CD8^+$ T-cells affects atherosclerosis development. The weight of the mice was unaffected, whereas cholesterol levels in serum were significantly increased by $CD8^+$ T-cell transfer of both Tc0 as well as Tc17 cells (Suppl. Figure 4D, E). Plaque size was assessed in the aortic root lesions of the hearts. Interestingly, neutral lipid staining of the lesions revealed the average lesion size of Tc17 transferred $CD8^+$ T-cells was equal to *Cd8a*$^{-/-}$*Ldlr*$^{-/-}$ mice that did not receive a transfer (Figure 5A). However, Tc0 mice that received the adoptively transferred Tc0 cells showed a 57.6% increase in lesion size, compared to the Tc17-treated group (Figure 5A). The increase in lesion size in the Tc0-treated group is partially due to an elevation in total macrophage accumulation, as MOMA positive are increased 2.8 fold, although this did not reach statistical significance. The relative plaque composition appeared to be similar in the Tc17- and Tc0-treated groups, as no change in the percentage of MOMA-positive, necrotic area, or collagen-positive area was observed (Figure 5B, C, D). Analysis of the VCAM-1^+ area in the caps of the lesion revealed a 1.5-fold increase in the Tc0-treated group, although this did not reach significance ($P=0.21$, Figure 5E).

DISCUSSION

$CD8^+$ T-cells play an important role in the adaptive immune response, responding to intracellular pathogens. Recently, $CD8^+$ T-cell subsets such as Tc1, Tc2, and Tc17, which are characterized by their cytokine production resulting from different environmental cues, have been reported to also play a role in various autoimmune disorders[21]. We report a large increase in Tc17 cells in the atherosclerotic lesion microenvironment specifically and show that adoptively transferred Tc17 cells do not contribute to the progression of atherosclerosis, while atherosclerotic lesion development was enhanced in Tc0-treated mice.

It is of particular interest to investigate the phenotype and function of $CD8^+$ T-cells within the lesion, as we have previously reported that $CD8^+$ T-cells can locally affect the lesion development and composition[46]. However, it is difficult to determine the presence of the different $CD8^+$ T-cell subsets within the lesional microenvironment based on their cytokine production, as the production of inflammatory cytokines produced by $CD8^+$ T-cells within the lesions is reduced[40]. Indeed, here we report a reduced percentage of IFN-γ^+ lesion-derived $CD8^+$ T-cells compared to their counterparts in the spleen and were hardly able to detect any IL-4, IL-5 or IL-17A production above background levels in the aorta of old *Apoe*$^{-/-}$ mice. Therefore, we set out to measure the transcription factors associated with the Tc1, Tc2, and Tc17 subsets instead. There is a reduced percentage of $CD8^+$ T-cells expressing T-bet in aortic lesions compared to splenic $CD8^+$ T-cells, suggesting that the pro-inflammatory Tc1 subset is not enriched in the lesion environment. However, we observed a modest increase in the percentage of cells expressing GATA3 in the lesions, implying an increase in Tc2 cells compared to lymphoid tissues.

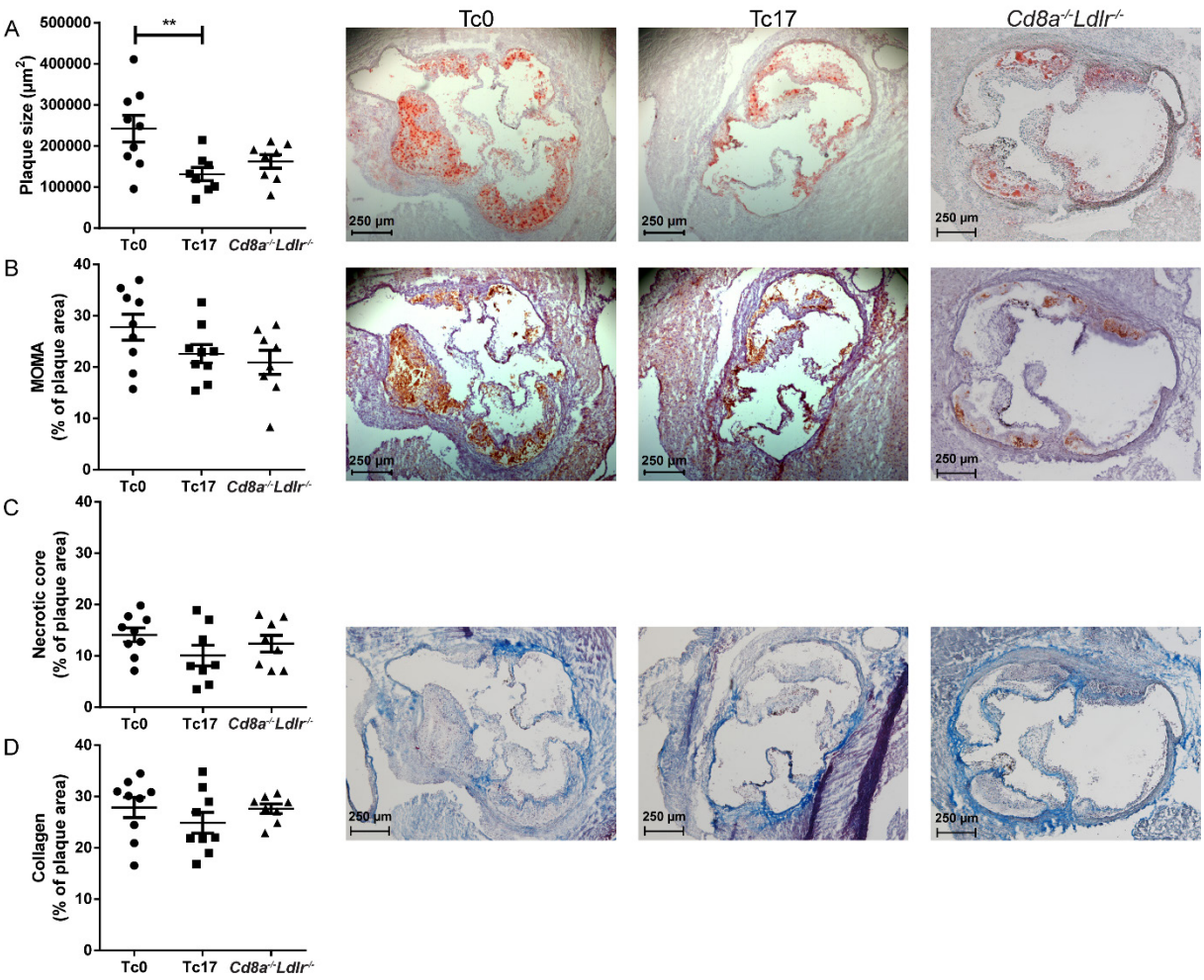

Figure 5. Adoptive transfer of Tc17 cells does not affect atherosclerotic lesion size, nor plaque composition, while a transfer of Tc0 cells accelerates lesion formation. (A) Quantification of lesion size in the aortic roots by Oil-red O staining and representative pictures of the lesions in *Cd8a*$^{-/-}$*Ldlr*$^{-/-}$ mice treated with Tc0 or Tc17 cells. (B) Quantification of relative monocyte/macrophage content in the aortic root lesions by MOMA staining and representative pictures of the lesions. (C) Quantification of relative necrotic core area in the aortic root lesions by Masson's Trichrome staining and representative pictures of the lesions. (D) Quantification of relative collagen content in the aortic root lesions by Sirius Red staining and representative pictures of the lesions. Individual data points and mean ± SEM, n=9 mice per group. Significance was determined by using an unpaired *t*-test. $P < 0.05$, $^{**}P < 0.01$, $^{***}P < 0.001$.

Strikingly, the percentage of cells expressing RORγt was strongly increased within the lesion microenvironment, which indicates a relative enrichment of Tc17 cells at the site of disease. It has previously been reported that 3 months of high-fat diet feeding in *Apoe*$^{-/-}$ mice results in increased IL-17A production by splenic T-cells[47], although the cell-type responsible for this increase was not specifically identified. We observed only very low percentages of IL-17^{+} CD8^{+} T-cells in the spleens of *Apoe*$^{-/-}$ mice, which were kept on a chow diet. Nonetheless, this study suggests that the inflammatory stimuli associated with the development of atherosclerosis may drive Tc17 skewing. Moreover, another analysis of the entire T-cell compartment showed an increase in IL-17A production in the aorta compared to the spleens of *Apoe*$^{-/-}$ mice fed a WTD for 15 weeks[16]. As there are enhanced levels of the Tc17-polarizing cytokines IL-1β and IL-6 in the plaque[48,49], the atherosclerotic environment in the lesion may indeed drive the local T-

cells to differentiate towards a Tc17 phenotype, or stimulate increased recruitment of these cells.

In vitro polarization of isolated $CD8^+$ T-cells from wild-type mice resulted in successful differentiation towards a Tc17 phenotype, as described previously using a similar differentiation protocol[41]. Some basal levels of IFN-γ were produced by both the Tc0 and Tc17 cells, which is in agreement with available data[33,41]. There was an increased expression of T-bet in the Tc0 subset compared to the Tc17 subset, which we hypothesize is due to the natural tendency of $CD8^+$ T-cells to differentiate towards an inflammatory effector phenotype upon the addition of IL-2, anti-CD3 and anti-CD28 antibodies[50]. Indeed, we found that the addition of anti-IFN-γ to the Tc0 conditions induced a great reduction in the T-bet expression, strengthening this hypothesis. However, upon adoptive transfer, Tc0 cells upregulated their expression of T-bet and IFN-γ production, indicating a switch towards the Tc1 phenotype. The Tc17 cells retained IL-17A production *in vivo*, though at lower levels than after *in vitro* differentiation. Finally, the RORγt expression was downregulated in these cells. Indeed, previous work using antigen-specific Tc17 cells has shown that these cells can convert to IFN-γ-producing cells, although they retain some of their IL-17A production[41]. Similar plasticity has been reported for $CD4^+$ Th17 subsets[51,52]. To date, the molecular mechanisms underlying these switches in phenotype remain unknown. However, the pro-inflammatory environment in the atherosclerotic mouse model may contribute to the increased production of IFN-γ, as hypercholesterolemia results in increased inflammatory responses[53,54]. As $CD8^+$ T-cells activated by using anti-CD3 and CD28 antibodies tend to differentiate towards an effector phenotype[50,55], it is likely that absence of anti-IFN-γ, that was present *in vitro*, as well as the inflammatory signaling induced by the WTD-feeding in our mouse model, drives the switch towards a Tc1 phenotype. Indeed, the Tc0 cells showed a similar phenotype *in vivo* to that which we observed for the splenic $CD8^+$ T-cells in the atherosclerotic *Apoe*$^{-/-}$ mice. Tc17 cells continued to produce IL-17A, but also gained the ability to produce IFN-γ. This may be explained by different transcriptional programs that are at work within this subset. IL-12, a cytokine known to be upregulated in atherosclerotic mice[56], is able to induce repressive epigenetic modification of the SOCS3 promoter. As SOCS3 is an essential mediator of IL-17 production, increased IL-12 levels in the blood can stimulate the conversion of Tc17 cells towards a mixed Tc1/Tc17 phenotype, associated with an increased IFN-γ production[57]. This is in agreement with our work, in which we observed maintenance of the Tc17 cytokine profile, but additional acquired characteristics of Tc1 cells. Previous work has demonstrated reciprocal plasticity between $CD4^+$ Th17 and Treg cells, since Th17 polarized cells can differentiate into Tregs *in vivo* and *vice versa*[58]. From this, it could be suggested that Tc17 cells can differentiate into regulatory $CD8^+$ T-cells via similar transcriptional mechanisms in our model. However, we observed no differences in FoxP3-expressing $CD8^+$ T-cells in our studies.

Of note, the Tc0 cells were more proliferative than their Tc17 counterparts. Possibly, the Tc0 cells resemble a more naïve phenotype as they are less fixed in their transcriptional program towards a certain phenotype. This enables them to proliferate more vigorously upon antigen recognition *in vivo*, compared to their more differentiated counterparts[59].

The injected $CD8^+$ T-cells were able to infiltrate the lesions *in vivo*, supporting the notion that local $CD8^+$ T-cell interactions in the lesions may have contributed to the observed differences between the Tc17- and Tc0-treated groups. However, we were unable to establish differences between the different treatment groups in expression of transcription factors or the production of cytokines by these aortic $CD8^+$ T-cells, as the cell numbers were too low to draw any significant conclusions about subsets within the population. Interestingly, no change in plaque size or composition could be identified between the Tc17-treated group and non-treated *Cd8a*$^{-/-}$*Ldlr*$^{-/-}$ mice, whereas transfer of Tc0 cells significantly increased the size of atherosclerotic

lesions. This strongly suggests Tc17 cells are not atherogenic and their enrichment in the plaques of CD8+ competent mice does not drive plaque progression and instability. Previous reports have shown an atheroprotective effect of IL-17, as increased expression of IL-17 reduced lesion development and neutralization of IL-17 accelerated atherosclerosis[18], which may explain the reduced pathogenicity of Tc17 cells. The proposed atheroprotective effect of IL-17 might contribute to the reduced pathogenicity of Tc17 cells. Alternatively, the reduced levels of IFN-γ produced by Tc17 may also account for this. IFN-γ is able to augment macrophage activation[60], which may, in turn, contribute to increased atherosclerosis development. IFN-γ$^{-/-}$*Apoe*$^{-/-}$ mice have been shown to display a large reduction in atherosclerosis compared to controls, associated with a decrease in lesion cellularity but an increase in lesional collagen content[36]. In another study, administration of IFN-γ to *Apoe*$^{-/-}$ mice resulted in a two-fold increase in lesion size, mediated by an increase in both T-cells as well as APCs[61]. CD8+ T-cell-derived IFN-γ has previously been shown to have limited impact on lesion size and stability[62], but this study was performed in lymphocyte-deficient *Apoe*$^{-/-}$ mice, which may overlook the effect of CD8+ T-cell-derived IFN-γ on CD4+ T-cells. We observed an increase in the total macrophage content of the lesions in the Tc0 group compared to the Tc17 and no transfer group, which could be mediated by the increased IFN-γ that is produced in these mice. In fact, we observed an increase in T-bet expressing Th1 CD4+ T-cells in the lesion microenvironment of the Tc0-treated mice. IFN-γ is an important regulator of T-bet expression within CD4+ T-cells[63-65], suggesting that the increase in Th1 cell population within the lesions of the Tc0-treated mice could be due to the increase in IFN-γ levels. In addition to the inflammatory effects of the adoptively transferred cells, this increase in the Th1 cell population within the lesions further promotes inflammation and atherogenesis, as these cells also display atherogenic functions[6]. Thus, the percentual increase in IL-17A, as well as the reduced proportion of IFN-γ production by the Tc17 cells compared to the Tc0 cells may have contributed to the reduce pathogenic effects observed here.

In conclusion, we have shown an enrichment in Tc17 cells in the plaque microenvironment of atherosclerotic mice. The enrichment of Tc17 cells does not affect the progression of atherosclerosis, in contrast to their Tc0 counterpart. These findings demonstrate the presence of different Tc subsets within atherosclerotic lesions and warrant further research into the function of these subsets in the plaque microenvironment.

FUNDING

This work was supported by the Netherlands CardioVascular Research Initiative: the Dutch Heart Foundation, Dutch Federation of University Medical Centres, the Netherlands Organisation for Health Research and Development, and the Royal Netherlands Academy of Sciences for the GENIUS project “Generating the best evidence-based pharmaceutical targets for atherosclerosis” [CVON2011-19].

CONFLICT OF INTEREST

None declared.

ACKNOWLEDGMENTS

We thank Servier for the free-of-charge use of their Medical Art images which can be found on https://smart.servier.com/

REFERENCES

1. van Dijk RA, Duinisveld AJ, Schaapherder AF, Mulder-Stapel A, Hamming JF, Kuiper J, de Boer OJ, van der Wal AC, Kolodgie FD, Virmani R, Lindeman JH. A change in inflammatory footprint precedes plaque instability: a systematic evaluation of cellular aspects of the adaptive immune response in human atherosclerosis. *Journal of the American Heart Association* 2015;**4**.
2. Huber SA, Sakkinen P, David C, Newell MK, Tracy RP. T helper-cell phenotype regulates atherosclerosis in mice under conditions of mild hypercholesterolemia. *Circulation* 2001;**103**:2610-2616.
3. Khallou-Laschet J, Caligiuri G, Groyer E, Tupin E, Gaston A-T, Poirier B, Kronenberg M, Cohen José L, Klatzmann D, Kaveri Srini V, Nicoletti A. The Proatherogenic Role of T Cells Requires Cell Division and Is Dependent on the Stage of the Disease. *Arteriosclerosis, thrombosis, and vascular biology* 2006;**26**:353-358.
4. Robertson AK, Hansson GK. T cells in atherogenesis: for better or for worse? *Arteriosclerosis, thrombosis, and vascular biology* 2006;**26**:2421-2432.
5. Grönberg C, Nilsson J, Wigren M. Recent advances on $CD4^+$ T cells in atherosclerosis and its implications for therapy. *European Journal of Pharmacology* 2017;**816**:58-66.
6. Buono C, Binder CJ, Stavrakis G, Witztum JL, Glimcher LH, Lichtman AH. T-bet deficiency reduces atherosclerosis and alters plaque antigen-specific immune responses. *Proc Natl Acad Sci U S A* 2005;**102**:1596-1601.
7. Frostegard J, Ulfgren AK, Nyberg P, Hedin U, Swedenborg J, Andersson U, Hansson GK. Cytokine expression in advanced human atherosclerotic plaques: dominance of pro-inflammatory (Th1) and macrophage-stimulating cytokines. *Atherosclerosis* 1999;**145**:33-43.
8. Ait-Oufella H, Salomon BL, Potteaux S, Robertson AK, Gourdy P, Zoll J, Merval R, Esposito B, Cohen JL, Fisson S, Flavell RA, Hansson GK, Klatzmann D, Tedgui A, Mallat Z. Natural regulatory T cells control the development of atherosclerosis in mice. *Nature medicine* 2006;**12**:178-180.
9. van Puijvelde GH, Hauer AD, de Vos P, van den Heuvel R, van Herwijnen MJ, van der Zee R, van Eden W, van Berkel TJ, Kuiper J. Induction of oral tolerance to oxidized low-density lipoprotein ameliorates atherosclerosis. *Circulation* 2006;**114**:1968-1976.
10. Binder CJ, Hartvigsen K, Chang M-K, Miller M, Broide D, Palinski W, Curtiss LK, Corr M, Witztum JL. IL-5 links adaptive and natural immunity specific for epitopes of oxidized LDL and protects from atherosclerosis. *The Journal of clinical investigation* 2004;**114**:427-437.
11. Miller AM, Xu D, Asquith DL, Denby L, Li Y, Sattar N, Baker AH, McInnes IB, Liew FY. IL-33 reduces the development of atherosclerosis. *The Journal of experimental medicine* 2008;**205**:339-346.
12. King VL, Szilvassy SJ, Daugherty A. Interleukin-4 deficiency decreases atherosclerotic lesion formation in a site-specific manner in female LDL $receptor^{-/-}$ mice. *Arteriosclerosis, thrombosis, and vascular biology* 2002;**22**:456-461.
13. Davenport P, Tipping PG. The role of interleukin-4 and interleukin-12 in the progression of atherosclerosis in apolipoprotein E-deficient mice. *Am J Pathol* 2003;**163**:1117-1125.
14. Foks AC, van Puijvelde GH, Bot I, ter Borg MN, Habets KL, Johnson JL, Yagita H, van Berkel TJ, Kuiper J. Interruption of the OX40-OX40 ligand pathway in LDL receptor-deficient mice causes regression of atherosclerosis. *J Immunol* 2013;**191**:4573-4580.
15. Erbel C, Chen L, Bea F, Wangler S, Celik S, Lasitschka F, Wang Y, Bockler D, Katus HA, Dengler TJ. Inhibition of IL-17A attenuates atherosclerotic lesion development in *Apoe*-deficient mice. *J Immunol* 2009;**183**:8167-8175.
16. Smith E, Prasad KM, Butcher M, Dobrian A, Kolls JK, Ley K, Galkina E. Blockade of interleukin-17A results in reduced atherosclerosis in apolipoprotein E-deficient mice. *Circulation* 2010;**121**:1746-1755.
17. van Es T, van Puijvelde GH, Ramos OH, Segers FM, Joosten LA, van den Berg WB, Michon IM, de Vos P, van Berkel TJ, Kuiper J. Attenuated atherosclerosis upon IL-17R signaling disruption in *Ldlr* deficient mice. *Biochem Biophys Res Commun* 2009;**388**:261-265.
18. Taleb S, Romain M, Ramkhelawon B, Uyttenhove C, Pasterkamp G, Herbin O, Esposito B, Perez N, Yasukawa H, Van Snick J, Yoshimura A, Tedgui A, Mallat Z. Loss of SOCS3 expression in T cells reveals a regulatory role for interleukin-17 in atherosclerosis. *The Journal of experimental medicine* 2009;**206**:2067-2077.
19. Joshi NS, Cui W, Chandele A, Lee HK, Urso DR, Hagman J, Gapin L, Kaech SM. Inflammation directs memory precursor and short-lived effector $CD8(^+)$ T cell fates via the graded expression of T-bet transcription factor. *Immunity* 2007;**27**:281-295.
20. Pipkin ME, Sacks JA, Cruz-Guilloty F, Lichtenheld MG, Bevan MJ, Rao A. Interleukin-2 and inflammation induce distinct transcriptional programs that promote the differentiation of effector cytolytic T cells. *Immunity* 2010;**32**:79-90.

21. Mittrucker HW, Visekruna A, Huber M. Heterogeneity in the differentiation and function of CD8($^+$) T cells. *Arch Immunol Ther Exp (Warsz)* 2014;**62**:449-458.
22. Grange M, Verdeil G, Arnoux F, Griffon A, Spicuglia S, Maurizio J, Buferne M, Schmitt-Verhulst AM, Auphan-Anezin N. Active STAT5 regulates T-bet and eomesodermin expression in CD8$^+$ T cells and imprints a T-bet-dependent Tc1 program with repressed IL-6/TGF-beta1 signaling. *J Immunol* 2013;**191**:3712-3724.
23. Wizel B, Nunes M, Tarleton RL. Identification of Trypanosoma cruzi trans-sialidase family members as targets of protective CD8$^+$ TC1 responses. *J Immunol* 1997;**159**:6120-6130.
24. Hamada H, Bassity E, Flies A, Strutt TM, Garcia-Hernandez Mde L, McKinstry KK, Zou T, Swain SL, Dutton RW. Multiple redundant effector mechanisms of CD8$^+$ T cells protect against influenza infection. *J Immunol* 2013;**190**:296-306.
25. Kemp RA, Ronchese F. Tumor-Specific Tc1, But Not Tc2, Cells Deliver Protective Antitumor Immunity. *The Journal of Immunology* 2001;**167**:6497.
26. Croft M, Carter L, Swain SL, Dutton RW. Generation of polarized antigen-specific CD8$^+$ effector populations: reciprocal action of interleukin (IL)-4 and IL-12 in promoting type 2 versus type 1 cytokine profiles. *J Exp Med* 1994;**180**:1715-1728.
27. Omori M, Yamashita M, Inami M, Ukai-Tadenuma M, Kimura M, Nigo Y, Hosokawa H, Hasegawa A, Taniguchi M, Nakayama T. CD8$^+$ T cell-specific downregulation of histone hyperacetylation and gene activation of the IL-4 gene locus by ROG, repressor of GATA. *Immunity* 2003;**19**:281-294.
28. Jia Y, Domenico J, Takeda K, Han J, Wang M, Armstrong M, Reisdorph N, O'Connor BP, Lucas JJ, Gelfand EW. Steroidogenic enzyme Cyp11a1 regulates Type 2 CD8$^+$ T cell skewing in allergic lung disease. *Proc Natl Acad Sci U S A* 2013;**110**:8152-8157.
29. Ning F, Takeda K, Schedel M, Domenico J, Joetham A, Gelfand EW. Hypoxia enhances CD8($^+$) TC2 cell-dependent airway hyperresponsiveness and inflammation through hypoxia-inducible factor 1alpha. *J Allergy Clin Immunol* 2019;**143**:2026-2037.e2027.
30. Hilvering B, Hinks TSC, Stöger L, Marchi E, Salimi M, Shrimanker R, Liu W, Chen W, Luo J, Go S, Powell T, Cane J, Thulborn S, Kurioka A, Leng T, Matthews J, Connolly C, Borg C, Bafadhel M, Willberg CB, Ramasamy A, Djukanović R, Ogg G, Pavord ID, Klenerman P, Xue L. Type-2 CD8$^+$ T lymphocytes responsive to PGD2 and LTE4 in severe eosinophilic asthma. *bioRxiv* 2018:247171.
31. Cho BA, Sim JH, Park JA, Kim HW, Yoo WH, Lee SH, Lee DS, Kang JS, Hwang YI, Lee WJ, Kang I, Lee EB, Kim HR. Characterization of effector memory CD8$^+$ T cells in the synovial fluid of rheumatoid arthritis. *Journal of clinical immunology* 2012;**32**:709-720.
32. Hamada H, Garcia-Hernandez MdlL, Reome JB, Misra SK, Strutt TM, McKinstry KK, Cooper AM, Swain SL, Dutton RW. Tc17, a unique subset of CD8$^+$ T cells that can protect against lethal influenza challenge. *Journal of immunology (Baltimore, Md : 1950)* 2009;**182**:3469-3481.
33. Huber M, Heink S, Grothe H, Guralnik A, Reinhard K, Elflein K, Hunig T, Mittrucker HW, Brustle A, Kamradt T, Lohoff M. A Th17-like developmental process leads to CD8($^+$) Tc17 cells with reduced cytotoxic activity. *Eur J Immunol* 2009;**39**:1716-1725.
34. Saxena A, Desbois S, Carrie N, Lawand M, Mars LT, Liblau RS. Tc17 CD8$^+$ T cells potentiate Th1-mediated autoimmune diabetes in a mouse model. *J Immunol* 2012;**189**:3140-3149.
35. Menon B, Gullick NJ, Walter GJ, Rajasekhar M, Garrood T, Evans HG, Taams LS, Kirkham BW. Interleukin-17$^+$ CD8$^+$ T cells are enriched in the joints of patients with psoriatic arthritis and correlate with disease activity and joint damage progression. *Arthritis & rheumatology (Hoboken, NJ)* 2014;**66**:1272-1281.
36. Gupta S, Pablo AM, Jiang X, Wang N, Tall AR, Schindler C. IFN-gamma potentiates atherosclerosis in *Apoe* knock-out mice. *The Journal of clinical investigation* 1997;**99**:2752-2761.
37. Cochain C, Koch M, Chaudhari SM, Busch M, Pelisek J, Boon L, Zernecke A. CD8$^+$ T Cells Regulate Monopoiesis and Circulating Ly6C-high Monocyte Levels in Atherosclerosis in Mice. *Circulation research* 2015;**117**:244-253.
38. Seijkens TTP, Poels K, Meiler S, van Tiel CM, Kusters PJH, Reiche M, Atzler D, Winkels H, Tjwa M, Poelman H, Slutter B, Kuiper J, Gijbels M, Kuivenhoven JA, Matic LP, Paulsson-Berne G, Hedin U, Hansson GK, Nicolaes GAF, Daemen M, Weber C, Gerdes N, de Winther MPJ, Lutgens E. Deficiency of the T cell regulator Casitas B-cell lymphoma-B aggravates atherosclerosis by inducing CD8$^+$ T cell-mediated macrophage death. *Eur Heart J* 2019;**40**:372-382.
39. Thiruvelselvan Ponnusamy KVS, Ramanjappa Manjunatha, Vijay V. Kakkar, Lakshmi Mundkur Circulating Th17 and Tc17 Cells and Their Imbalance with Regulatory T Cells Is Associated with Myocardial Infarction in Young Indian Patients. *World Journal of Cardiovascular Diseases* 2015;**5**:373-387.

40. van Duijn J, van Elsas M, Benne N, Depuydt M, Wezel A, Smeets H, Bot I, Jiskoot W, Kuiper J, Slütter B. CD39 identifies a microenvironment-specific anti-inflammatory CD8⁺ T-cell population in atherosclerotic lesions. *Atherosclerosis* 2019;**285**:71-78.
41. Yen HR, Harris TJ, Wada S, Grosso JF, Getnet D, Goldberg MV, Liang KL, Bruno TC, Pyle KJ, Chan SL, Anders RA, Trimble CL, Adler AJ, Lin TY, Pardoll DM, Huang CT, Drake CG. Tc17 CD8$^+$ T cells: functional plasticity and subset diversity. *J Immunol* 2009;**183**:7161-7168.
42. Lewis MD, de Leenheer E, Fishman S, Siew LK, Gross G, Wong FS. A reproducible method for the expansion of mouse CD8$^+$ T lymphocytes. *J Immunol Methods* 2015;**417**:134-138.
43. den Haan JM, Lehar SM, Bevan MJ. CD8(+) but not CD8(-) dendritic cells cross-prime cytotoxic T cells in vivo. *The Journal of experimental medicine* 2000;**192**:1685-1696.
44. Kolbus D, Ljungcrantz I, Soderberg I, Alm R, Bjorkbacka H, Nilsson J, Fredrikson GN. TAP1-deficiency does not alter atherosclerosis development in *Apoe*$^{-/-}$ mice. *PloS one* 2012;**7**:e33932.
45. Elhage R, Gourdy P, Brouchet L, Jawien J, Fouque MJ, Fievet C, Huc X, Barreira Y, Couloumiers JC, Arnal JF, Bayard F. Deleting TCR alpha beta$^+$ or CD4$^+$ T lymphocytes leads to opposite effects on site-specific atherosclerosis in female apolipoprotein E-deficient mice. *Am J Pathol* 2004;**165**:2013-2018.
46. van Duijn J, Kritikou E, Benne N, van der Heijden T, van Puijvelde GH, Kroner MJ, Schaftenaar FH, Foks AC, Wezel A, Smeets H, Yagita H, Bot I, Jiskoot W, Kuiper J, Slutter B. CD8$^+$ T-cells contribute to lesion stabilization in advanced atherosclerosis by limiting macrophage content and CD4$^+$ T-cell responses. *Cardiovasc Res* 2018.
47. Madhur MS, Funt SA, Li L, Vinh A, Chen W, Lob HE, Iwakura Y, Blinder Y, Rahman A, Quyyumi AA, Harrison DG. Role of interleukin 17 in inflammation, atherosclerosis, and vascular function in apolipoprotein e-deficient mice. *Arteriosclerosis, thrombosis, and vascular biology* 2011;**31**:1565-1572.
48. Reiss AB, Siegart NM, De Leon J. Interleukin-6 in atherosclerosis: atherogenic or atheroprotective? *Clinical Lipidology* 2017;**12**:14-23.
49. Libby P. Interleukin-1 Beta as a Target for Atherosclerosis Therapy: Biological Basis of CANTOS and Beyond. *Journal of the American College of Cardiology* 2017;**70**:2278-2289.
50. Hughes DP, Baskar D, Urban FF, Friedman MS, Braun TM, McDonagh KT. Fate and function of anti-CD3/CD28-activated T cells following adoptive transfer: IL-2 promotes development of anti-tumor memory T cells in vivo. *Cytotherapy* 2005;**7**:396-407.
51. Lee YK, Turner H, Maynard CL, Oliver JR, Chen D, Elson CO, Weaver CT. Late developmental plasticity in the T helper 17 lineage. *Immunity* 2009;**30**:92-107.
52. Bending D, De la Pena H, Veldhoen M, Phillips JM, Uyttenhove C, Stockinger B, Cooke A. Highly purified Th17 cells from BDC2.5NOD mice convert into Th1-like cells in NOD/SCID recipient mice. *The Journal of clinical investigation* 2009;**119**:565-572.
53. Centa M, Prokopec KE, Garimella MG, Habir K, Hofste L, Stark JM, Dahdah A, Tibbitt CA, Polyzos KA, Gistera A, Johansson DK, Maeda NN, Hansson GK, Ketelhuth DFJ, Coquet JM, Binder CJ, Karlsson MCI, Malin S. Acute Loss of Apolipoprotein E Triggers an Autoimmune Response That Accelerates Atherosclerosis. *Arteriosclerosis, thrombosis, and vascular biology* 2018;**38**:e145-e158.
54. Chyu KY, Lio WM, Dimayuga PC, Zhou J, Zhao X, Yano J, Trinidad P, Honjo T, Cercek B, Shah PK. Cholesterol lowering modulates T cell function in vivo and in vitro. *PloS one* 2014;**9**:e92095.
55. Gunnlaugsdottir B, Maggadottir SM, Ludviksson BR. Anti-CD28-induced co-stimulation and TCR avidity regulates the differential effect of TGF-beta1 on CD4$^+$ and CD8$^+$ naive human T-cells. *International immunology* 2005;**17**:35-44.
56. Lee TS, Yen HC, Pan CC, Chau LY. The role of interleukin 12 in the development of atherosclerosis in *Apoe*-deficient mice. *Arteriosclerosis, thrombosis, and vascular biology* 1999;**19**:734-742.
57. Satoh T, Tajima M, Wakita D, Kitamura H, Nishimura T. The development of IL-17/IFN-gamma-double producing CTLs from Tc17 cells is driven by epigenetic suppression of Socs3 gene promoter. *Eur J Immunol* 2012;**42**:2329-2342.
58. Lee GR. The Balance of Th17 versus Treg Cells in Autoimmunity. *Int J Mol Sci* 2018;**19**:730.
59. Geginat J, Lanzavecchia A, Sallusto F. Proliferation and differentiation potential of human CD8^{$^+$} memory T-cell subsets in response to antigen or homeostatic cytokines. *Blood* 2003;**101**:4260.
60. Held TK, Weihua X, Yuan L, Kalvakolanu DV, Cross AS. Gamma interferon augments macrophage activation by lipopolysaccharide by two distinct mechanisms, at the signal transduction level and via an autocrine mechanism involving tumor necrosis factor alpha and interleukin-1. *Infection and immunity* 1999;**67**:206-212.
61. Whitman SC, Ravisankar P, Elam H, Daugherty A. Exogenous Interferon-γ Enhances Atherosclerosis in Apolipoprotein E−/− Mice. *The American Journal of Pathology* 2000;**157**:1819-1824.

62. Kyaw T, Winship A, Tay C, Kanellakis P, Hosseini H, Cao A, Li P, Tipping P, Bobik A, Toh BH. Cytotoxic and proinflammatory CD8$^+$ T lymphocytes promote development of vulnerable atherosclerotic plaques in *Apoe*-deficient mice. *Circulation* 2013;**127**:1028-1039.
63. Lighvani AA, Frucht DM, Jankovic D, Yamane H, Aliberti J, Hissong BD, Nguyen BV, Gadina M, Sher A, Paul WE, O'Shea JJ. T-bet is rapidly induced by interferon-γ in lymphoid and myeloid cells. 2001;**98**:15137-15142.
64. Cope A, Le Friec G, Cardone J, Kemper C. The Th1 life cycle: molecular control of IFN-gamma to IL-10 switching. *Trends Immunol* 2011;**32**:278-286.
65. Smeltz RB, Chen J, Ehrhardt R, Shevach EM. Role of IFN-gamma in Th1 differentiation: IFN-gamma regulates IL-18R alpha expression by preventing the negative effects of IL-4 and by inducing/maintaining IL-12 receptor beta 2 expression. *J Immunol* 2002;**168**:6165-6172.

SUPPLEMENTARY FIGURES

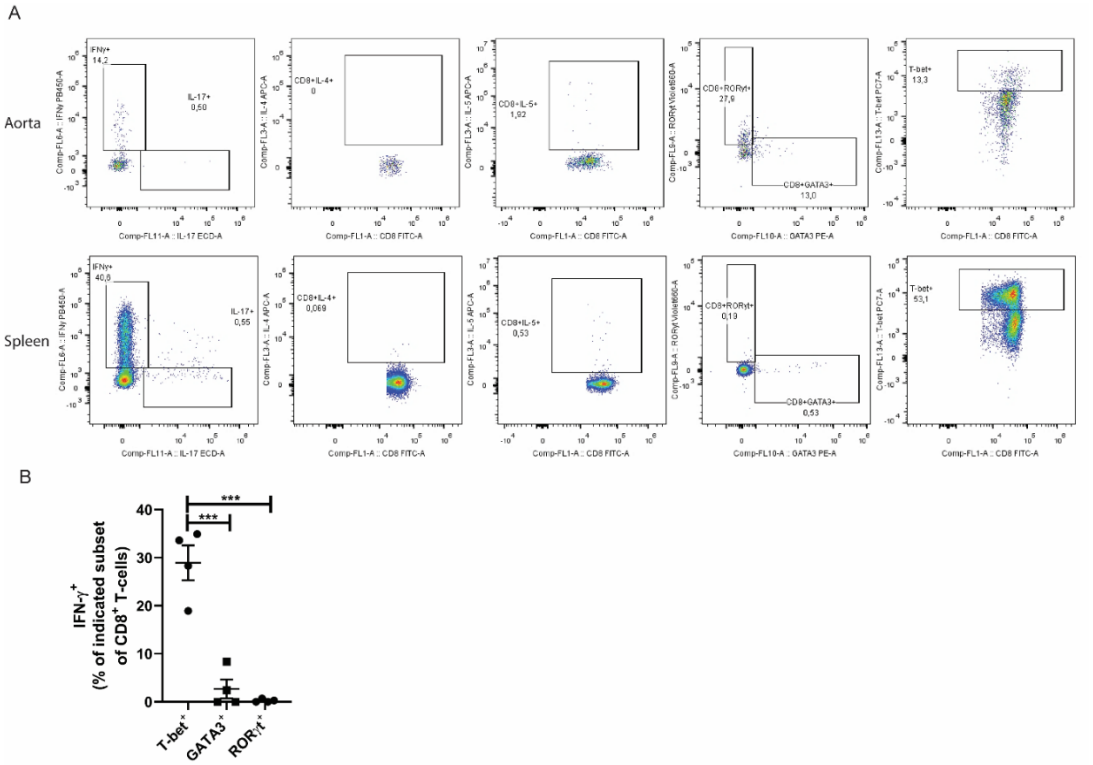

Supplementary Figure 1: IFN-γ production in murine atherosclerotic lesions is restricted to T-bet-expressing CD8$^+$ T-cells. (A) Representative images of flow cytometry results shown in figure 1. Cytokine-positive populations were gated based on unstimulated controls. (B) Flow cytometric analysis of IFN-γ production by T-bet$^+$, GATA3$^+$ and RORγt$^+$ CD8$^+$ T-cells in the aortas of *Apoe*$^{-/-}$ mice stimulated for 3.5 h with PMA and ionomycin. Cells were pre-gated on live, Thy1.2$^+$ CD8$^+$ T-cells and the indicated transcription factors. Individual data points and mean±SEM of n=4 *Apoe*$^{-/-}$ mice that were 46 to 49 weeks old. Significance was determined by using a one-way ANOVA with Bonferroni's multiple comparisons. *P < 0.05, **P < 0.01, ***P < 0.001.

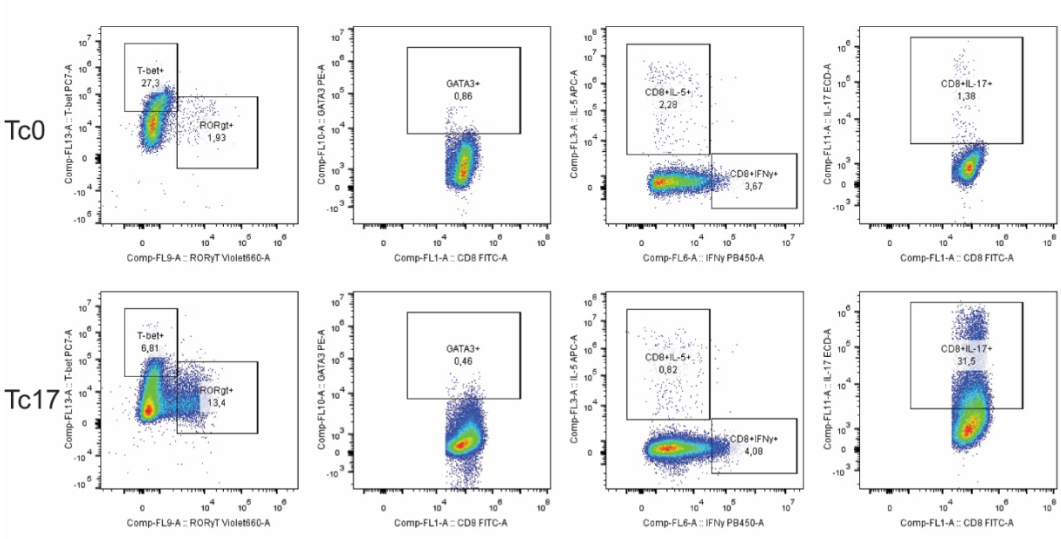

Supplementary Figure 2 : Representative images of flow cytometry results shown in figure 2. Cytokine-positive populations were gated based on unstimulated controls.

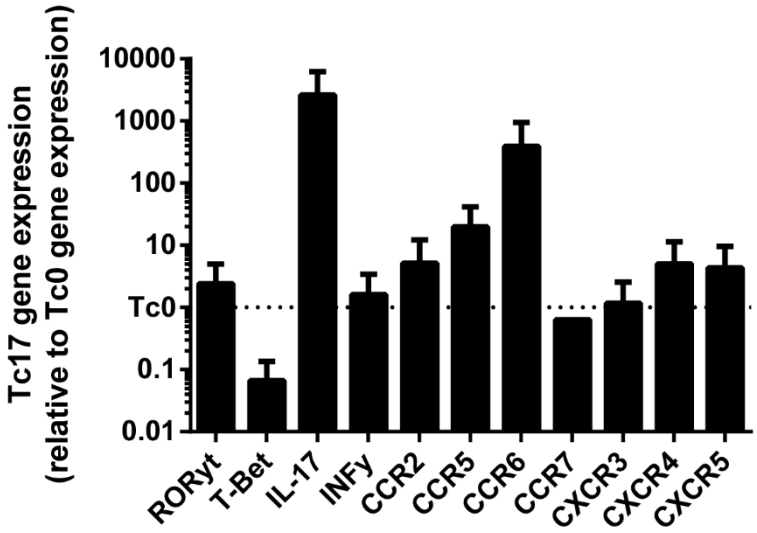

Supplementary figure 3: Transcription profile of Tc0 and Tc17 cells. Quantative PCR analysis of RORγt, T-Bet, IL-17, INF-γ, CCR2, CCR5, CCR6, CCR7, CXCR3, CXCR4 and CXCR5 in Tc0 and Tc17 cells. Gene expression was normalized for β-actin gene expression and represented as relative to Tc0. Bar graph including mean ± SEM, n=2 measurements.

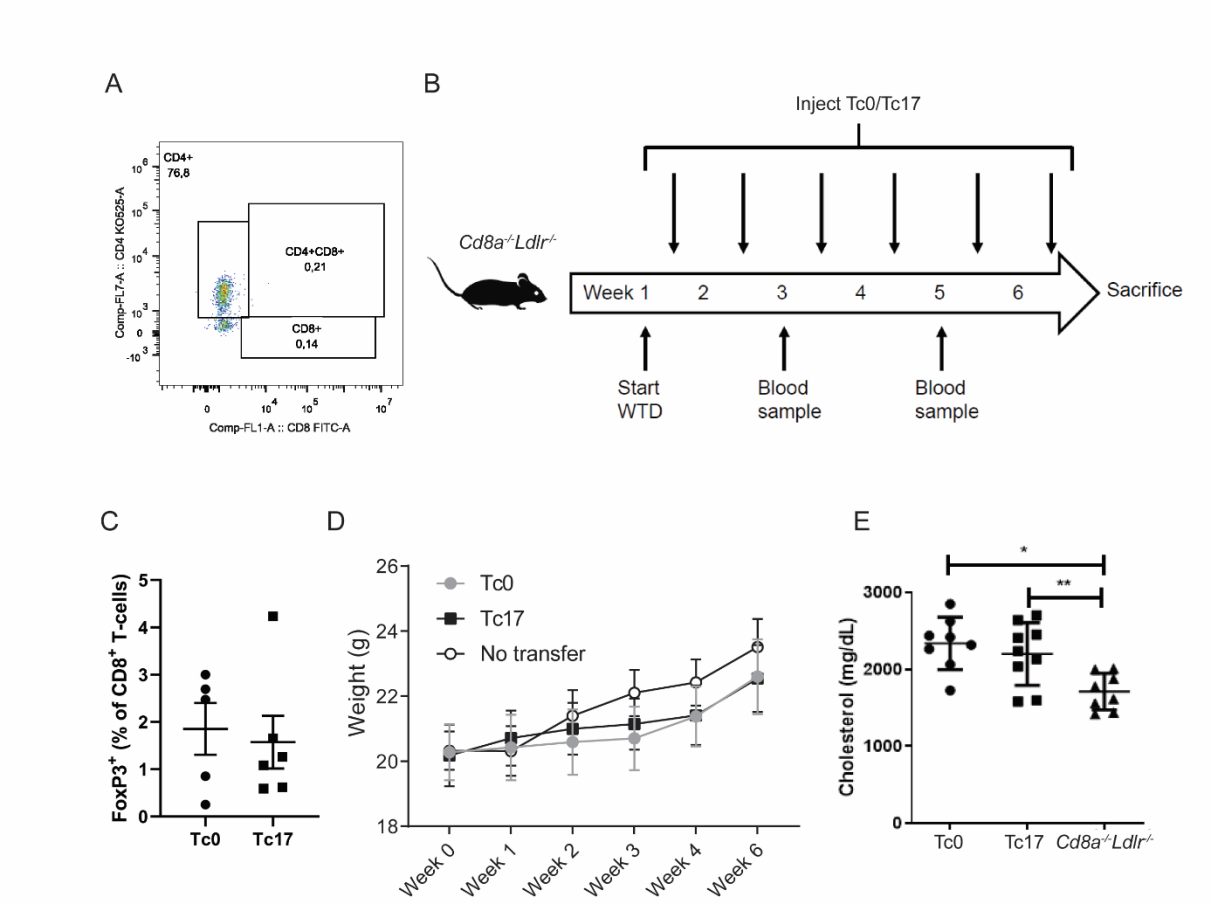

Supplementary Figure 4: Adoptive transfer of Tc0 or Tc17 cells into *Cd8a$^{-/-}$Ldlr$^{-/-}$* mice does not result in any significant differences in weight or serum cholesterol. (A) Representative facs plot of the blood of a *Cd8a$^{-/-}$Ldlr$^{-/-}$* mice showing CD4 and CD8^{+} staining at baseline bleeding. Plot was pregated on Live, Thy1.2^{+} cells. (B**)** Schematic overview of the setup of the adoptive transfer experiment (C) Flow cytometric analysis of FoxP3^{+} CD8^{+} T-cells in the spleens of the *Cd8a$^{-/-}$Ldlr$^{-/-}$* mice that received the adoptive transfer of Tc0 or Tc17 cells at the time of sacrifice. Significance was determined by using an Mann-Whitney test. (D) Body weights of *Cd8a$^{-/-}$Ldlr$^{-/-}$* mice that received adoptive transfer of Tc0 or Tc17 cells once weekly, mean ± SEM. Significance was determined by using a two-way ANOVA with Bonferroni's multiple comparisons (E) Serum cholesterol levels at sacrifice. Significance was determined by using an unpaired *t*-test. Individual data points and mean ± SEM, n=9 mice per group.

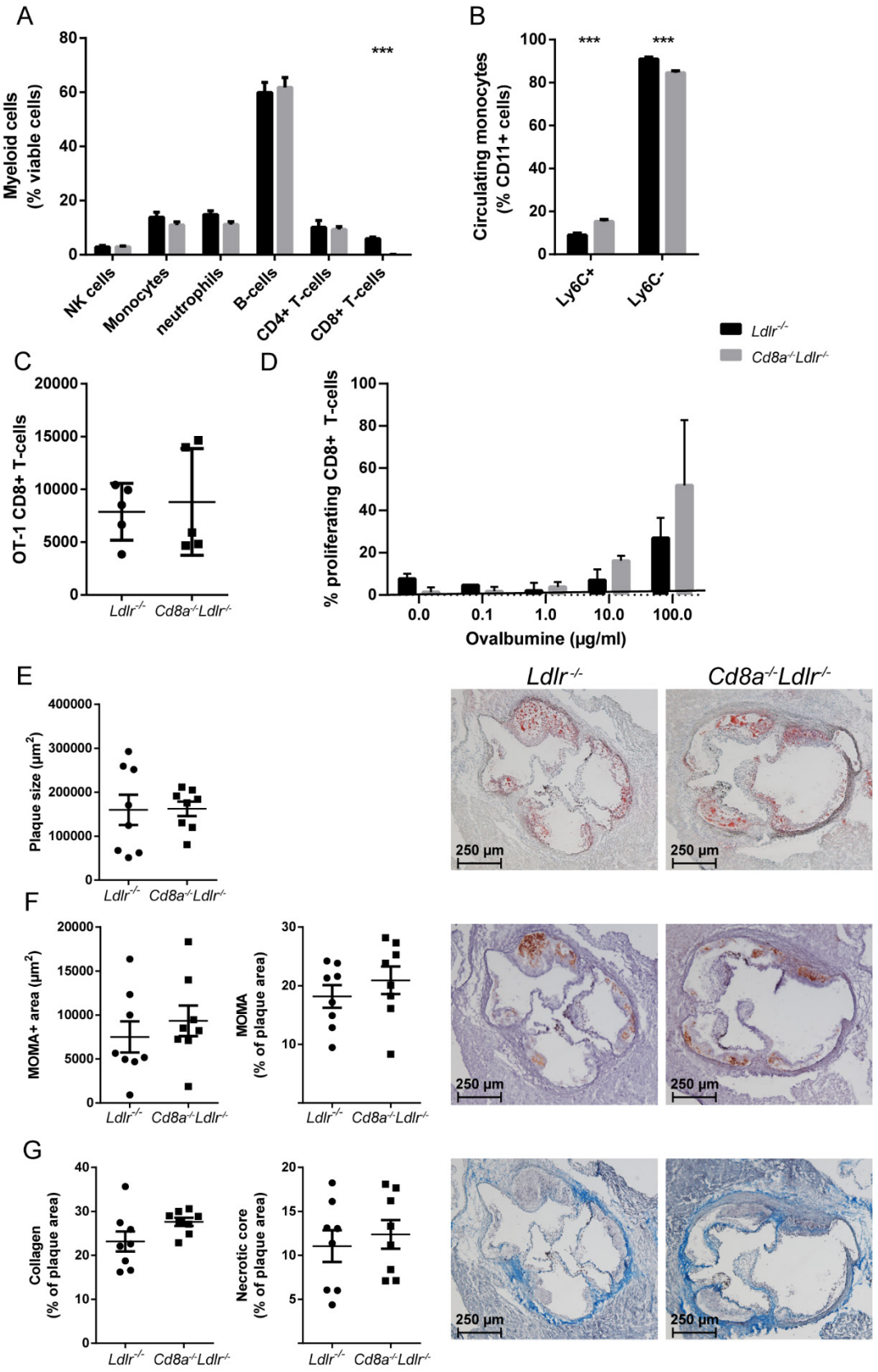

Supplementary figure 5: leukocyte populations and atherosclerotic lesion development is not affected by CD8+ deletion on a *Ldlr-/-* background. Flow cytometric analysis of (A) NK-cells (NK1.1+), monocytes (CD11b+, Ly6G-), neutrophils (CD11b+, Ly6G+), B-cells (CD19+), CD4 T-cells (CD4+), CD8+ T-cells (CD8+), and (B) the activation level of monocytes (Ly6C+ or Ly6C- monocytes) in blood of *Cd8a-/-Ldlr-/-* mice or *Ldlr-/-* mice after 6 weeks of WTD. *(Continued)*

Cells were pre-gated on live cells (A), or live, CD11b$^+$, Ly6G- cells (B). (C) *In vivo* CD8$^+$ T-cell expansion after an adoptive transfer of 50.000 ovalbumin specific CD8$^+$ T-cell (OT-I) and vaccination with 100µg ovalbumin and 50µg poly I:C into *Ldlr*$^{-/-}$ and *Cd8a*$^{-/-}$*Ldlr*$^{-/-}$ mice. Expansion of transferred CD8$^+$ T-cells was evaluated by FACS analysis (CD45.1$^+$ CD8$^+$ T-cells). (D) *In vitro* expansion of OT-I T-cells co-cultured with DCs, exposed to different concentrations of ovalbumin and lipopolysaccharide. (E) Quantification of lesion size in the aortic roots by Oil-red O staining and representative pictures of the lesions in *Cd8a*$^{-/-}$*Ldlr*$^{-/-}$ mice and *Ldlr*$^{-/-}$ mice. (F) Quantification of absolute and relative monocyte/macrophage content in the aortic root lesions by MOMA staining and representative pictures of the lesions. (G) Quantification of relative collagen content and necrotic core in the aortic root lesions by Trichrome staining and representative pictures of the lesions. Data is displayed in a bar graph plotted as mean ± SEM, n=8 mice per group. Significance was determined by using a multiple *t*-test with a false discovery rate approach (*P < 0.01, **P < 0.001)(A, B) or an unpaired *t*-test (C, D, E) (*P < 0.05, **P < 0.01, ***P < 0.001)(D, E, F).

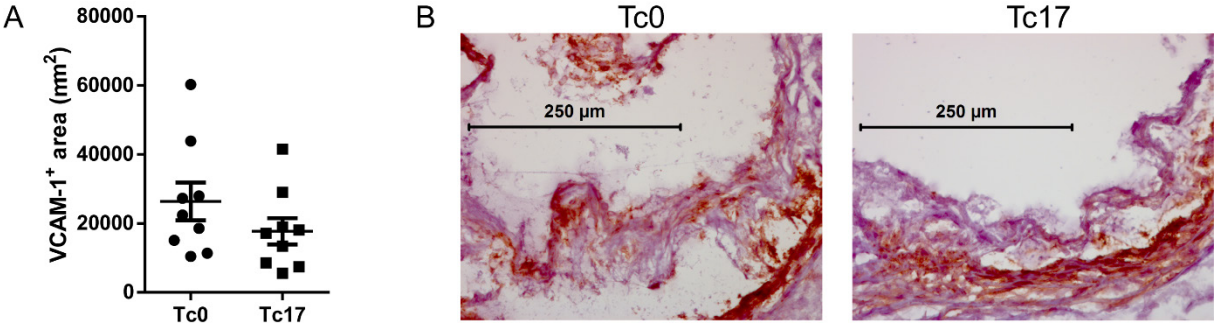

Supplementary figure 6: Tc0 Treated mice show a trend towards increased VCAM-1 expression, compared to Tc17 treated mice. (A) Quantification of absolute VCAM-1$^+$ area in the caps of the aortic root lesions by VCAM-1 staining. (B) Representative pictures of the lesions. Significance was determined by a two-tailed Student's t-test.

SUPPLEMENTARY TABLES

Antibody	Fluorochrome	Clone	Supplier
CD4	APC	GK1.5	BioLegend
CD4	PerCP	RM4-5	BD Biosciences
CD4	V500	RM4-5	BD Biosciences
CD8	eFluor450	53-6.7	eBioscience
CD8	FITC	53-6.7	eBioscience
CD8	PE-Texas Red	5H10	Invitrogen
EOMES	APC	Dan11mag	eBioscience
FoxP3	eFluor450	FJK-16s	eBioscience
GATA3	PE	16E10A23	eBioscience
IFN-γ	eFluor450	XMG1.2	eBioscience
IL-17A	PE	TC11-18H10.1	Biolegend
IL-17A	PEdazzle594	TC11-18H10.1	Biolegend
IL-5	APC	TRFK5	Biolegend
Ki-67	FITC	SolA15	eBioscience
RORγt	BV650	Q31-378	BD Biosciences
Thy1.2	PeCy7	53-2.1	Biolegend
Thy1.2	PerCP-cy5.5	53-2.1	Biolegend
T-bet	PeCy7	eBio4B10	eBioscience
Fixable viability dye	eFluor780	-	eBioscience

Supplementary table 1 : Antibodies used for flow cytometric analysis.

Transcript	Forward primer	Reverse primer
B-actin	cttctttgcagctccttcgttgccg	aatacagcccggggagcatcgtc
RORγt	ctgcaagactcatcgacaaggcctc	tccttatagagtggagggaaggcgg
T-bet	agtgactgcctaccagaacgcagag	ccaggtggcgaggggacact
IL-17a	tgatcaggacgcgcaaacatgagtc	aagtccttggcctcagtgtttggac
INFy	ccttcttcagcaacagcaaggcga	gcgctggacctgtgggttgt
CCR2	gctgcctgcaaagaccagaagag	tgccgtggatgaactgaggtaaca
CCR5	aattctttggactgaataactgca	tggatcgggtatagactgagctt
CCR6	caggggcaacttacaaatcctgggt	gcaggcgtggttctctatgtggatg
CCR7	cgtgctggtggtggctctcct	accgtggtattctcgccgatgtagtc
CXCR3	agttcccaaccacaagtgccaaagg	ccagaagaaaggcaaagtccgaggc
CXCR4	ggtgatcctggtcatgggtt	tgacaggtgcagccggta
CXCR5	cgagctgagtggctatctctct	agaggtcactgcggaactttac

Supplementary table 2. Primer list. List of primers used during the qPCR.